

*Letter to the Editor***Submillimetre maps of the edge-on galaxy NGC 891**F.P. Israel¹, P.P. van der Werf¹, and R.P.J. Tilanus^{2,3}¹ Sterrewacht Leiden, P.O. Box 9513, 2300 RA Leiden, The Netherlands² Joint Astronomy Centre, 660 N. A'ohoku Pl., Hilo, Hawaii, 96720, USA³ Netherlands Foundation for Research in Astronomy, P.O. Box 2, 7990 AA Dwingeloo, The Netherlands

Received 20 April 1998 / Accepted 17 March 1999

Abstract. Broadband continuum images of the edge-on galaxy NGC 891 at 850 μm and 450 μm are presented. These images are very similar to the 1300 μm and CO line images. With respect to the 850 μm continuum, CO is strongest in the so-called molecular ring¹, and weakest at the largest radii sampled. Inside the molecular ring, the CO/850 μm ratio is somewhat less than in the ring, but higher than in the remainder of the disk. The integrated infrared emission from NGC 891 is dominated by small particles shortwards of 100 μm . Longwards of 100 μm , the emission can be equally well fitted by a single population of large dust grains at 21 K, or a bimodal population of grains at temperatures of 18 K and 27 K. The circumnuclear disk is at a temperature of at least 50 K, and probably much higher.

Key words: galaxies: active – galaxies: individual: NGC 891 – galaxies: ISM – galaxies: nuclei – infrared: galaxies

1. Introduction

NGC 891 is a bright, non-interacting spiral galaxy (SA(s)b: De Vaucouleurs et al. 1976). It is very nearly edge-on ($i > 88^\circ$, $PA = 23^\circ$; Sofue & Nakai 1993). NGC 891 is one of the major members of the NGC 1023 group and its distance is estimated to be 9.5 Mpc for $H_0 = 75 \text{ km s}^{-1} \text{ Mpc}^{-1}$, making for a scale of $22''/\text{kpc}$ or $46 \text{ pc}''$. Many authors have remarked on the apparent similarity between NGC 891 and the Milky Way. The interstellar medium in the disk of NGC 891 has been the subject of several studies, notably radio continuum (Allen et al. 1978; Sukumar & Allen 1991), HI (Sancisi & Allen 1979; Rupen 1991), dust (Howk & Savage 1997); CO (García-Burillo et al. 1992; Scoville et al. 1993; Sofue & Nakai 1993; García-Burillo & Guélin 1995; Sakamoto et al. 1997) and CI (Gerin & Phillips 1997). Far-infrared dust emission was observed by IRAS (see Wainscoat et al. 1987; Rice et al. 1988), and at $\lambda = 1.3 \text{ mm}$ by Guélin et al. 1993. In this paper we present further observations of the submillimeter dust emission from NGC 891 with the new SCUBA submillimeter continuum array detector.

Send offprint requests to: F.P. Israel

Correspondence to: israel@strw.leidenuniv.nl

2. Observations

The SCUBA 850 and 450 μm images were obtained in 1997 September on the JCMT¹. SCUBA employs two arrays of cooled bolometers, each covering a field of about $2'3$. The respective filters used have central frequencies of 347 GHz and 677 GHz respectively; both filters have a bandwidth of 30 GHz. We observed three fields on NGC 891 (center, northeast and southwest) in so-called ‘jiggle-mode’ in order to cover the whole galaxy. Chopping distance was $2'$ perpendicular to the major axis of the galaxy. Total integration time for the three fields was 128 minutes. Reduction was performed in the standard manner. Photometric calibration was achieved by skydip analysis and mapping of the standard star CRL 618. More complete details of the instrument as well as observing and reduction methods can be found in Holland et al. (1998) and Jenness et al. (1998), as well as on the world-wide web (www.jach.hawaii.edu). The resulting images are shown in Fig. 1. Especially in the 450 μm image, residual noise is seen at the SCUBA field edges; this should be discounted.

3. Results*3.1. Total submillimetre spectrum and dust content*

Guélin et al. (1993) have fitted two dust components at 15 K and 30 K to their 1.3 mm flux and the IRAS 100 μm flux. From our maps, we have determined integrated flux-densities $S_{850} = 4.8 \pm 0.6 \text{ Jy}$ and $S_{450} = 39 \pm 7 \text{ Jy}$. The observations through the 850 μm filter include emission from the $J=3-2$ ^{12}CO line. In similar beams, the first three CO transitions occur in intensity ratios of 1:0.75:0.4 (see García-Burillo et al. 1992; Gerin & Phillips 1997). From this, we estimate an integrated $J=3-2$ CO contribution of 0.22 Jy to the measured 850 μm flux-density. Corrected for this contribution, the dust continuum emission becomes $S_{850} \approx 4.6 \text{ Jy}$. The $J=6-5$ ^{12}CO transition is at the edge of the 450 μm filter; we expect its contribution to the ob-

¹ The James Clerk Maxwell Telescope is operated by the Joint Astronomy Centre on behalf of the Particle Physics and Astronomy Research Council of the United Kingdom, the Netherlands Organisation for Scientific Research and the National Research Council of Canada

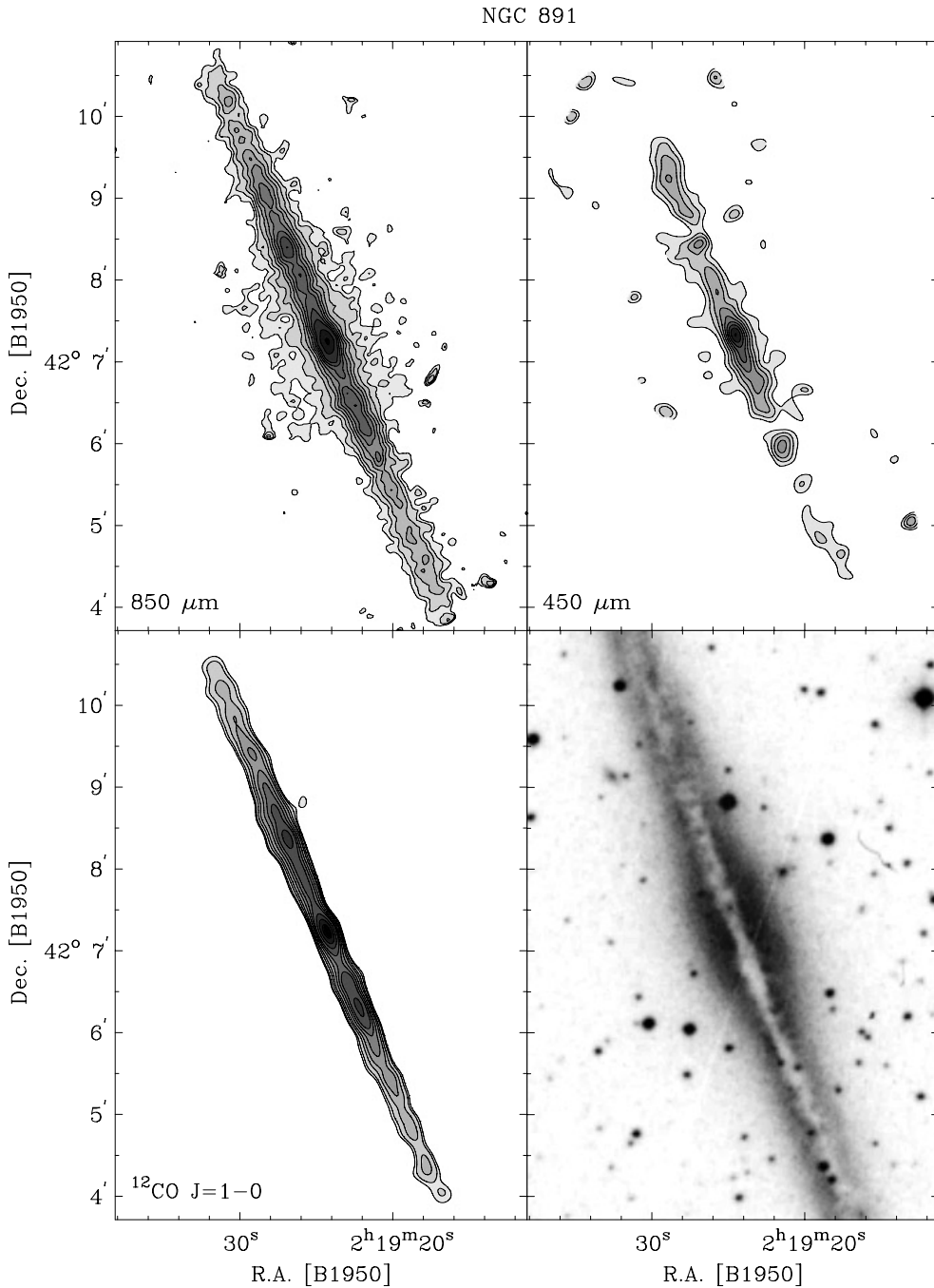


Fig. 1. Submillimeter continuum images at $13''$ resolution of NGC 891 at $850\ \mu\text{m}$ (top left) and $450\ \mu\text{m}$ (top right). Contour levels are 15, 30, 50, 75, 100, 125, 150, 175, 200, 250 and 300 mJy/beam ($850\ \mu\text{m}$), 500, 750, 1000, 1250, 1500, 1750, 2000, 2250 and 2500 mJy/beam ($450\ \mu\text{m}$). For comparison, the interferometric $J=1-0$ ^{12}CO map obtained by Scoville et al. (1993) is included at bottom left, and an optical image at bottom right.

served flux to be negligible. With $S_{1300} = 0.73$ Jy (Guélin et al. 1993), and the IRAS flux densities $S_{12} = 6$ Jy, $S_{25} = 7$ Jy, $S_{60} = 80$ Jy and $S_{100} = 196$ Jy (Wainscoat et al. 1987; Rice et al. 1988; Young et al. 1989), the infrared/submillimeter spectrum of NGC 891 is now well-determined.

Assuming a dust emissivity proportional to λ^{-2} , we have fitted these flux-densities with various dust temperatures.

(i). Longwards of $100\ \mu\text{m}$, a good fit is obtained with a *single* dust temperature $T_d \approx 21$ K. However, this fit leaves the mid-infrared fluxes and most of the $60\ \mu\text{m}$ flux to be explained. The interstellar dust models by Désert, Boulanger & Puget (1990)

suggest that virtually all of the $12\ \mu\text{m}$ flux and about 50% of the $25\ \mu\text{m}$ flux is attributable to PAH particles. This implies a ratio $F_{25}/F_{60} = 0.1$ for the remaining very-small grain (VSG) component which suggests an average VSG size somewhat larger than in the Solar Neighbourhood, i.e. about 10 nm instead of 7 nm (see Désert et al. 1993). We have used Eq. (2) from Guélin et al. (1993) to calculate the total hydrogen mass associated with the radiating dust (assuming $b(Z/Z_\odot) = 1.6$) and find $M_H = 3 \times 10^9 M_\odot$.

(ii). Next, we assume that the $12-1300\ \mu\text{m}$ spectrum is described by the dust model of Désert et al. (1990), with big-grain dust

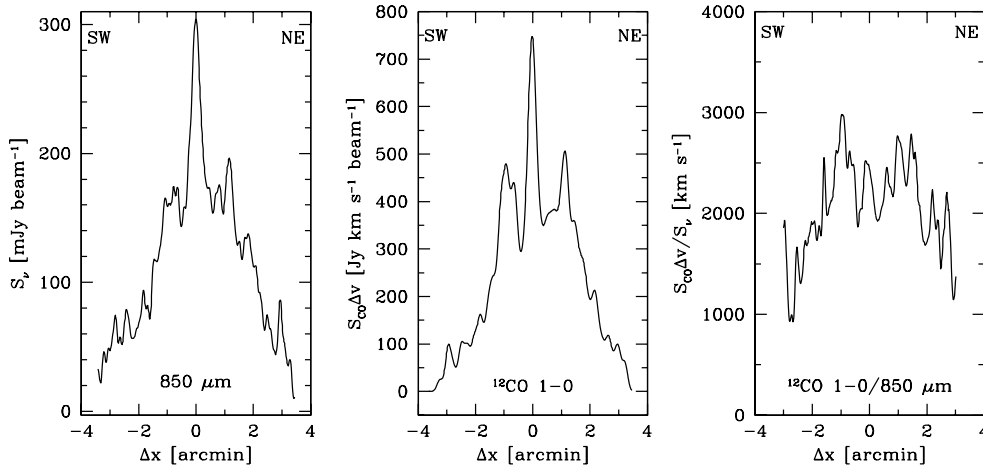


Fig. 2. Radial distribution of $850\ \mu\text{m}$ (left), $J=1-0\ ^{12}\text{CO}$ (center) emission in NGC 891 and the ratio of observed CO/ $850\ \mu\text{m}$ emission (right). Profiles show emission at $13''$ resolution along the major axis.

radiating at two different temperatures. With dust temperatures $T_{\text{wd}} = 28 \pm 2\ \text{K}$ and $T_{\text{cd}} = 18 \pm 1\ \text{K}$, close to the values assumed by Guélin et al. (1993), calculated fluxes reproduce the observed values to better than 20% over the full wavelength range. At $850\ \mu\text{m}$, we find flux-densities of $1.2\ \text{Jy}$ (VSG), $0.55 \pm 0.15\ \text{Jy}$ (warm dust) and $3.1 \pm 0.2\ \text{Jy}$ (cold dust). From this, we obtain $M_{\text{H}}(\text{warm}) = 3.3 \pm 1.1 \times 10^8\ M_{\odot}$ and $M_{\text{H}}(\text{cold}) = 3.6 \pm 0.4 \times 10^9\ M_{\odot}$, or a total mass $M_{\text{rH}}(\text{total}) = 3.9 \pm 0.3 \times 10^9\ M_{\odot}$, slightly less than that estimated by Guélin et al. (1993). The ratio $M_{\text{H}}(\text{warm})/M_{\text{H}}(\text{cold}) = 0.1 \pm 0.04$ is higher than surmised by Guélin et al. (1993).

Because the dust emission is a strong function of temperature, the temperatures are relatively well-determined, depending on the choice of one or two temperature components. As is clear from the above, the choice of temperature model has relatively little effect on the derived mass. Following Guélin et al. (1993), we adopt $M(\text{HI}) = 2.5 \times 10^9\ M_{\odot}$ so that $M(\text{H}_2) = 1.4 \times 10^9\ M_{\odot}$. this yields a conversion factor $X = N(\text{H}_2)/I_{\text{CO}} \approx 7 \times 10^{19}\ \text{mol cm}^{-2}\ (\text{K km s}^{-1})^{-1}$, somewhat less than found by Guélin et al. (1993) and Gerin & Phillips (1997) and substantially less than the canonical value. Assuming $M(\text{HI})_{\text{tot}} = 3.7 \times 10^9$ (Allen & Sancisi, 1979; Rupen 1991) and all H_2 to be sampled, the overall ratio of molecular to atomic hydrogen is 0.38, the molecular gas fraction is 0.20 and within $R = 16.5\ \text{kpc}$, the total gas fraction, including helium, is 5%. The first two values are similar to those found for the Milky Way and for dwarf irregular galaxies (Israel 1997).

3.2. Radial distributions

The structure of CO and dust continuum emission along the major axis can be roughly described by three components: the very compact central source at (a circumnuclear disk – García-Burillo et al. 1992; Scoville et al. 1993; Sofue & Nakai 1993), a ‘molecular ring’ between $R = 40''$ and $R = 120''$ (2–6 kpc) and the extended disk traceable out to $R = 200''$ (9 kpc). Given the edge-on configuration of NGC 891, the various peaks in the emission are most likely spiral arms seen tangentially. This

includes the bright inner peaks which may well be due to bright spiral arms encircling the bulge rather than a ring.

As Fig. 1 shows, the $850\ \mu\text{m}$ (and $450\ \mu\text{m}$) continuum image is virtually identical to the $J=1-0$ CO image. This is in line with the close resemblance of the $1.3\ \text{mm}$ to the $J=2-1\ ^{12}\text{CO}$ distribution (Guélin et al. 1993) and indeed to the $^3P_1 - ^3P_0$ CI distribution (Gerin & Phillips 1997) and the 6 cm continuum emission (see Allen et al. 1978). This is further illustrated by the radial distributions shown in Fig. 2. Fig. 2c shows $J=1-0$ CO/ $850\ \mu\text{m}$ emission ratios of 1500 for the central peak and 2000 for the molecular ring peaks (or inner spiral arm tangential points), dropping to 1300 for the inner region inside the ‘ring’.

Although decreasing signal-to-noise ratios introduce increasingly large relative errors in the outer disk ratios, there appears to be a steady decrease in this ratio, in the outer disk dropping to 70% of the value at $R = \pm 2'$, just outside the molecular ring. The run of the $450/850/1300\ \mu\text{m}$ intensities with radius provides no support for significant dust temperature gradients. We propose that the high ratio of the molecular ring primarily reflects a higher CO surface filling factor. If the inner spiral arms contain a rich population of dense CO clouds, this will quite naturally produce a relatively high CO filling factor (hence a high ratio in Fig. 2c) at the arm tangential points. High line-of-sight CO optical depths are suggested by the $^{12}\text{CO}/^{13}\text{CO}$ ratio of 2.5 for the ring (Sakamoto et al. 1997).

The decrease of the CO/ $850\ \mu\text{m}$ ratio with increasing distance to the center parallels the radial drop in CO emissivity shown by Scoville et al. (1993) and the even steeper decrease of ^{13}CO emission (Sakamoto et al. 1997), resulting in a $^{12}\text{CO}/^{13}\text{CO}$ gradient increasing from 5 just outside the molecular ring to about 15 in the outer disk. The latter interpret this as a steep radial decrease of the dense gas fraction, so that we may expect the effects of photo-dissociation processes to increase radially. This appears to be confirmed by the observed major axis distributions of [CI] (Gerin & Phillips 1997) and [CII] (Madden et al. 1994).

The central region is quite different. Virtually all major axis profiles exhibit a pronounced dip inside the molecular ring, onto which the compact emission from the circumnuclear disk is su-

perposed. This suggests that the region *inside the molecular ring*, i.e. the region within $R = 2$ kpc corresponding to the bulge of NGC 891, contains *little* interstellar material except for the circumnuclear disk of radius 600 pc. The emission observed towards the center mostly represents material in the molecular ring with a smaller contribution from the outer disk. The cavity appears to be filled by very hot ($T = 3.6 \times 10^6$ K) X-ray-emitting gas, extending into the molecular ring (Bregman & Pildis 1994). West of the nucleus, an X-ray jet feature is seen. This, and the presence of a nuclear disk suggests that NGC 891 has a mildly active nucleus. We have attempted to separate the nuclear continuum emission peak from the more extended emission. We find fluxes $S_{1300} = 55$ mJy, $S_{850} = 230$ mJy and $S_{450} = 2200$ mJy. Corrected for CO line contributions (García-Burillo et al. 1992; Gerin & Phillips 1997), these reduce to 40, 190 and 2200 mJy respectively. Although these fluxes are relatively uncertain, they define a spectrum considerably steeper than that of the galaxy as a whole. If all dust radiates at the same temperature, we find $T_d > 50$ K, at least twice as high as the whole galaxy under the same assumption. A similar temperature ($T_k > 40$ K was derived by Sakamoto et al. (1997) for the molecular gas in the nuclear disk.

4. Conclusions

We have mapped the submillimetre emission from the edge-on galaxy NGC 891 at wavelengths of $850 \mu\text{m}$ and $450 \mu\text{m}$. The appearance of both maps is very similar to those obtained by others at $1300 \mu\text{m}$ and in the ^{12}CO line. The integrated infrared spectrum of NGC 891 shortwards of $100 \mu\text{m}$ is dominated by emission from PAH particles and very small dust grains. Longwards of $100 \mu\text{m}$ emission from large dust grains dominates. The emission spectrum between $100 \mu\text{m}$ and $1300 \mu\text{m}$ can be fitted equally well by a single population of grains at a temperature of 20 K, or a bimodal population of grains at temperatures of 18 K and 27 K. In either case, we find a total hydrogen mass of the order of $3 \times 10^9 M_\odot$, somewhat less than estimated by Guélin et al. (1993), but close enough to be consistent. As a consequence, we confirm their conclusion that the CO-to- H_2 conversion ratio in NGC 891 is substantially less (by a factor of 2–4) than the canonical values frequently used.

The distribution of the various ISM components as a function of distance to the center of the galaxy of these ISM components can be described as roughly gaussian, with a strong central peak and several lesser peaks in the disk superposed. The central peak originates in a compact circumnuclear disk

($R = 15''$ or 0.7 kpc; see García-Burillo et al. 1992; Scoville et al. 1993). The compact circumnuclear disk is embedded in soft X-ray emission and is at a temperature of at least 40 K, and probably significantly higher. The lesser peaks probably mark spiral arms seen tangentially. Although the submillimetre continuum emission from dust and the line emissions from CO and CI show very similar distributions, their intensity ratios vary across the galaxy. Towards the central region CO and especially CI are relatively weak compared to the dust emission at $850 \mu\text{m}$. In the so-called ‘molecular ring’ we find the reverse: CO and CI are relatively strong. At greater distances to the center, the CO to dust emission ratio decreases, whereas the CI to dust emission ratio increases. This behaviour may be explained by an ‘empty’ bulge region, by greater CO and CI surface filling factors in tangential spiral arms, and by an increase in photo-dissociation effects at greater radial distances due to an increasing paucity of dense molecular clouds.

References

- Allen R.J., Baldwin J.E., Sancisi R., 1978 A&A62, 397
 Bregman J.N., Pildis R.A., 1994 ApJ420, 570
 De Vaucouleurs G., De Vaucouleurs A., Corwin H.C., 1976, *Second Reference Catalogue of Bright Galaxies*, University of Texas Press, Austin (RC2)
 Désert F.-X., Boulanger F., Puget J.L., 1990 A&A237, 215
 García-Burillo S., Guélin M., Cernicharo J., Dahlem M., 1992 A&A266, 21
 García-Burillo S., Guélin M., 1995 A&A299, 657
 Gerin M., Phillips T.G., 1997 ESA-IRAM Conference on the FIRST Mission, in press
 Guélin M., Zylka R., Mezger P.G., et al. 1993 A&A279, L37
 Holland W.S., Cunningham C.R., Gear W.K., et al. 1998 SPIE, in press
 Howk J.C., Savage B.D., 1997 AJ114 246
 Israel F.P., 1997 A&A328, 471
 Jenness T., Lightfoot J.F., 1998 *ASP Conf. Series* ***, in press
 Rice W., Lonsdale C.J., Soifer B.T., et al. 1988 ApJS68, 91
 Rupen M.P., 1991 AJ102, 48
 Sakamoto S., Handa T., Sofue Y., Honma M., Sorai K., 1997 ApJ475, 134
 Sancisi R., Allen R.J., 1979 A&A74, 73
 Scoville N.Z., Thakkar D., Carlstrom J.E., Sargent A.I., 1993, ApJ404, L59
 Sofue Y., Nakai N., 1993 PASJ45, 139
 Sukumar S., Allen R.J., 1991 ApJ382, 100
 Wainscoat R.J., de Jong T., Wesselius P.R., 1987 A&A181, 225
 Young J.S., Xie S., Kenney J.D.P., Rice W.L., ApJS70, 699